Proceedings of the Institute of Acoustics

DETERMINATION OF THE DIRECTIVITY OF A PLANAR NOISE SOURCE BY MEANS OF NEAR-FIELD ACOUSTICAL HOLOGRAPHY

D J Oldham and M A Rowell

Department of Architecture and Building Engineering,
The University of Liverpool, PO BOX 147
Liverpool, L69 3BX

1. INTRODUCTION

One of the major problems encountered when trying to measure the directional characteristics of an acoustic source, is that the measurement must be performed in the far-field. This usually implies a distance from the source of many times its 'size'. To overcome this problem, many researchers [1][2] have proposed that allow measurements made in the near-field of a source to be used in calculating it's far-field characteristics. Methods such as these require a measurement of pressure and/or velocity to be made over an array of points close to a source. This set of discrete values is then used in a Helmholtz type integral to calculate the pressure at a particular far-field position. The main problem of methods of this type is that performing the integral for each far-field point is computationally very time consuming. In this presentation, a method is proposed using Near-field Acoustical Holography (NAH) [3][4] to calculate the far-field pressure due to a source. Because of the use of the FFT algorithm in the calculations, the far-field directivity of a source can be calculated much more efficiently. Also, using broadband holographic techniques [5][6], a broadband (1/3 or whole octave) far-field directivity can be calculated.

1.1 Definition of Directivity

The definition of far-field directivity used in this work is as follows:

$$D(\theta,\phi) = \frac{I(R,\theta,\phi)}{I_h} \qquad (1)$$

where: $I(R,\theta,\phi)$ is the far-field intensity by the source
θ is the polar angle
ϕ is the azimuthal angle
I_h is the intensity which would be produced by the source if it radiated omni-directionally into a half space i.e. $I_h = W/2\pi R^2$

2 THE CALCULATION OF THE FAR-FIELD INTENSITY

The far-field intensity in Eq. (1), $I(R,\theta,\Phi)$ is obtained from the far-field pressure $p(R,\theta,\Phi)$, which is calculated using the following well-known formula, relating the far-field pressure of a source and the Fourier transform of the source velocity, V_z:

$$p(R,\theta,\Phi) = -jk\rho c \frac{e^{jkR}}{2\pi R} V_z(k_x,k_y) \qquad (2)$$

where: $k_x = k\sin\theta\cos\Phi$ and
$k_y = k\sin\theta\sin\Phi$
for $k_x^2 + k_y^2 \leq k^2$ i.e. inside the radiation circle.

This formulation of the far-field pressure is equivalent to the one given in Ref. [3]. For low-frequencies, there will only be a few points of the discrete data set inside the radiation circle, giving rise to a poorly defined far-field pressure. The method used in this work to greatly increase the definition of the far-field pressure is a 'sampling expansion' method of interpolation, outlined by Papoulis [7]. This method uses an interpolating filter to calculate the value of a function H at some frequency k', from a set of 2N discrete values $H(\mu.dk)$ thus:

$$H(k') = \sum_{\mu=0}^{2N-1} H(\mu.dk)\ K_\mu(k' - \mu.dk) \qquad (3)$$

where K_μ is the interpolating filter function given by the following:

$$K_\mu(k' - \mu.dk) = \frac{\sin(N\cdot dx(k' - \mu.dk))\ e^{jdx(k'-\mu dk)/2}}{2N\sin(dx(k' - \mu.dk)/2)} \qquad (4)$$

where dx and dk are the spacing of the hologram grid in real and k-space respectively, and $k_{x\mu} = \mu.dk$ is the k-space sample frequency.

For the case of two-dimensions, as in NAH, a double summation is used, following the notation of Veronesi and Maynard [4] thus:

$$H(k_x,k_y) = \sum_\mu \sum_\nu H(k_{x\mu},k_{y\nu})\ K_\mu(k_x-k_{x\mu})\ K_\nu(k_y-k_{y\nu}) \qquad (5)$$

where H represents the magnitude of the far-field pressure. If the far-field pressure is required in one direction ($k_x = 0$ or $k_y = 0$, corresponding to the xz or yz planes), and not over the whole hemisphere, Eq. (5) reduces to a one-dimensional summation which is much less computationally demanding than the double summation.

3. THE CALCULATION OF THE POWER

The acoustic power W, of the source, required for the calculation of directivity (see Eq. (1)) can be calculated in one of two ways:

3.1 Integration In The Far-field

The first method of calculating the acoustic power is to integrate far-field intensity over a hemisphere in front of the source:

$$W = R^2 \int_0^{\pi/2} d\theta \int_0^{\pi} \sin\theta \, I(R,\theta,\phi) \, d\phi \qquad (6)$$

In NAH this integral is reformatted to be performed over the radiation circle, $k_x^2 + k_y^2 \leq k^2$, thus:

$$W = \frac{R^2}{k} \int_{-k}^{k} dk_y \int_{-(k^2-k_y^2)^{\frac{1}{2}}}^{(k^2-k_y^2)^{\frac{1}{2}}} \frac{I(k_x,k_y)}{(k^2-k_x^2-k_y^2)^{\frac{1}{2}}} \, dk_x \qquad (7)$$

which enables Eq. (7) to be calculated using a simple double summation. The advantage of this method is that the far-field intensity is already known.

3.2 Integration Over the Source Plane

The second method for calculating the power of the source, is to integrate the product of the pressure and the complex conjugate normal particle velocity over the source plane, $z = 0$ [8]. This takes more time than the far-field method, as both the real-space pressure and velocity of the source have to be determined.

4. NUMERICAL SIMULATION

This method for calculating directivity has been tested for two numerically simulated sources, over a range of frequencies and hologram 'measurement' parameters. The two sources used were as follows:

* A circular piston
* A simply supported panel

The piston radius used was 0.5m, the panel dimensions were 1m x 1m, and the panel mode is (3,1), following the notation of Wallace [9]. For the results shown here, the hologram 'measurement' parameters were as follows:

Hologram aperture (L) = 2.2m
Number of points (N) = 64
Hologram distance (Z_h) = 0.03m

Fig. (1) show the directivity index = $10\text{Log}_{10}(D(\theta,\phi))$ for the piston for ka values of 1,5,10 and 40, corresponding to approximate frequencies of 100, 500, 1000 and 4000 Hz, in the xz-plane. As can be seen, the agreement between the directivity calculated from NAH and the theoretical directivity is generally very good, apart from at low frequencies, ka = 1. It can be seen from Fig. (2) that the same conclusion also applies for the panel source, for ka/2 = 1,5,10 and 40.

The poor estimate of the source directivity at low frequencies ($ka \leq 1$) is due to the sampled pressure over the finite hologram aperture being a poor representation of the true pressure over an infinite domain.

For large values of the polar angle, ($\theta \rightarrow \pi/2$), where the far-field position approaches the plane of the source, it can be seen that the calculated directivity decreases compared to the theoretical directivity. This decrease in the calculated directivity is due to the nature of the k-space Greens function [4] used in the reconstruction of the k-space source velocity, causing the far-field intensity to be underestimated as θ approaches $\pi/2$.

A result from a broadband simulation can be seen in Fig. (3). This shows the 1kHz 1/3 octave theoretical and calculated directivity for the piston source. The 1/3 octave directivity indeces were synthesized by summing the narrowband far-field intensity and power estimates for frequencies from 900 Hz to

1120 Hz in steps of 20Hz (12 narrow band values in all). As can be seen the agreement is very good.

5. THE EXPERIMENTS

For experimental verification of the method, a computer controlled xy-traverse was designed and constructed, with a maximum scan area of approximately 2.5m x 2.5m. A single scanning microphone with a phase reference signal was used to measure the complex pressure at each grid-point, using a dual channel FFT analyzer. The signal used to excite the source was a multisine signal as used by Strong [6]. This signal is broadband in nature, but at the same time deterministic, and hence the averaging time required per grid-point is small compared with that for a normal broadband noise signal.

5.1 Directivity of a Loudspeaker

To test the method, the directivity of a 12" (30cm) diameter loudspeaker in a baffle was measured using a 1.1m x 1.1m, 32 x 32 point grid, and compared with the directivity calculated from a direct measurement of the far-field SPL at 3m and the power using an intensity scan close to the loudspeaker. Figure (4) shows this comparison for the 2500Hz 1/3 octave. As can be seen, the agreement is good. It must be noted that the direct measurement of far-field SPL could be in error for large angles from the normal, due to the proximity of the side walls in the semi-anechoic room used as the receiving room.

5.2 Directivity of Homogeneous and Non-Homogeneous Panels

Using this method, the directivity index of a variety of panels, both flat and corrugated has been measured. Figure (5) shows the directivity index at 4kHz for a 6mm thick aluminium panel measuring 0.9m x 1.2m. As can be seen the panel exhibits the "lobes" as predicted by Shen and Oldham [10]. Figure (6) shows the directivity index for a trapezoidally corrugated thin (0.7mm) steel panel of similar dimensions to the homogeneous aluminium panel. Even though panels of this type have a low critical frequency in a direction parallel to the corrugations (the yzplane in the figures), the panel exhibits no pronounced directional lobes.

6. CONCLUSIONS

A method has been demonstrated for measuring the directivity of planar sources. The method gives excellent agreement with theory for mid and high frequencies. The method does not give reliable results at low frequencies, due to the low number of

points inside the radiation circle, and due to the low accuracy of the power calculation. Work is continuing on the development of a 2D "zoom" fast Fourier transform, to change the resolution of the k-space quantities, such that the radiation circle encompasses the majority of the k-space sample values, for all source frequencies.

7. ACKNOWLEDGEMENTS

The authors would like to thank the Science and Engineering Research Council for funding this work.

8. REFERENCES

[1] D.D.Baker, "Determination of Far-field Characteristics of Large Underwater Sound Transducers from Near-field Measurements", J.A.S.A., 34 (1962) pp.1737-1744.

[2] C.W.Horton and G.S.Innis Jr., "The Computation of Far-field Radiation Patterns from Measurements made near the Source", J.A.S.A., 33 (1961), pp.877-880.

[3] J.D.Maynard, E.G.Williams and Y.Lee, "Near-field Acoustical Holography (NAH) I: Theory of Generalised Holography and the Development of NAH", J.A.S.A., 78 (1985), pp.1395-1413.

[4] W.A.Veronesi and J.D.Maynard, "Near-field Acoustical Holography (NAH) II: Holographic Reconstruction Algorithms and Computer Implementation", J.A.S.A., 81 (1987), pp.1307-1322.

[5] K.B.Washburn and E.G.Williams, "Measurement Techniques and Results in Broadband Generalised Near-field Acoustical Holography", NOISE-CON 87, Proc. of the Nat. Conf. Noise Control Engineering, (1987), pp.649-654.

[6] W.Y.Strong, "Multiple Frequency Source Excitation with Near-field Acoustical Holography", NOISE-CON 87, Proc. of the Nat. Conf. Noise Control Engineering, (1987), pp.641-648.

[7] A.Papoulis, "Signal Analysis", McGraw-Hill, (1977) pp.162-164.

[8] E.G.Williams and J.D.Maynard, "Numerical Evaluation of the Rayleigh Integral for Planar Radiators using the FFT", J.A.S.A., 72 (1982), pp.2020-2030.

[9] C.E.Wallace, "Radiation Resistance of a Rectangular Panel", J.A.S.A., 51 (1972), pp.946-952.

[10] Y.Shen and D.J.Oldham, "A Scale Model Investigation of Sound Radiation from Building Elements", J.S.V., 91 (1983), pp.331-350.

DIRECTIVITY OF A PLANAR SOURCE

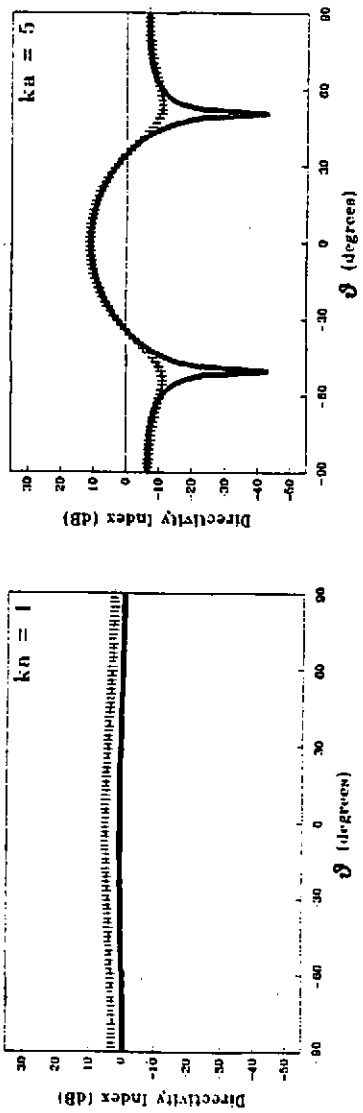

Figure 1: Numerical simulation for the piston source; theory, + NAH

DIRECTIVITY OF A PLANAR SOURCE

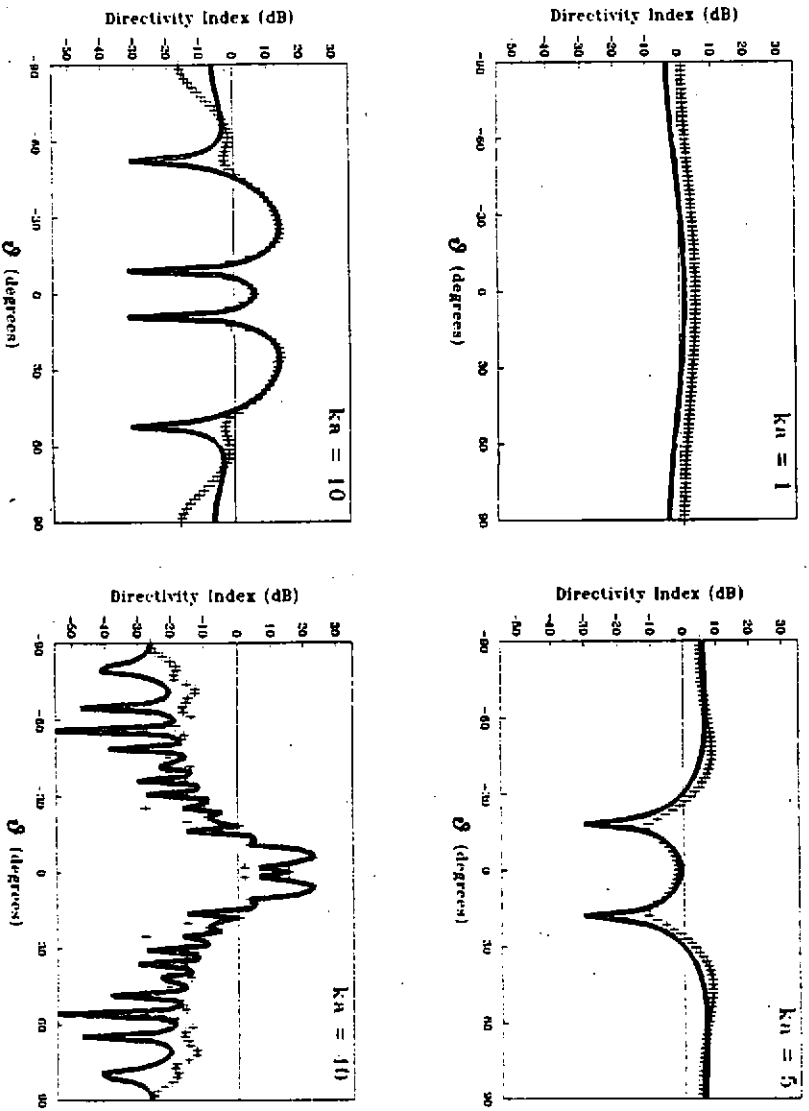

Figure 2: Numerical simulation for the panel source
- theory, + NAH

DIRECTIVITY OF A PLANAR SOURCE

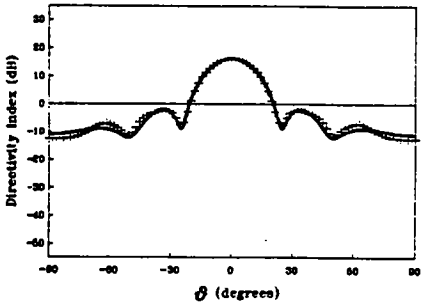

Figure 3: Numerical simulation for the piston source, 1kHz 1/3 octave; - theory, + NAH

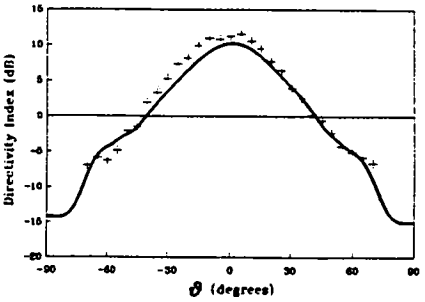

Figure 4: Comparison of the directivity index of a loudspeaker in the 2.5kHz 1/3 octave band for the direct (+) and NAH (-) methods of measurement

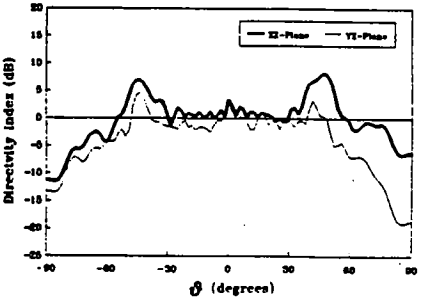

Figure 5: The directivity index of a homogeneous aluminium panel in the 4kHz 1/3 octave band

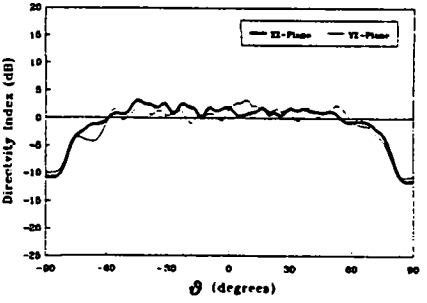

Figure 6: The directivity index of a trapezoidally corrugated steel panel in the 4kHz 1/3 octave band